Collision-Driven Negative-Energy Waves and the Weibel Instability of a Relativistic Electron Beam in a Quasineutral Plasma

Anupam Karmakar,[1] Naveen Kumar,[1] Gennady Shvets,[2] Oleg Polomarov,[2] and Alexander Pukhov[1,*]

[1]Institut für Theoretische Physik I, Heinrich-Heine-Universität, Düsseldorf, 40225, Germany

[2]Department of Physics and Institute for Fusion Studies, University of Texas at Austin, One University Station, Austin, Texas 78712, USA

(Received 1 July 2008; published 15 December 2008)

A new model describing the Weibel instability of a relativistic electron beam propagating through a resistive plasma is developed. For finite-temperature beams, a new class of negative-energy magnetosound waves is identified, whose growth due to collisional dissipation destabilizes the beam-plasma system even for high beam temperatures. We perform 2D and 3D particle-in-cell simulations and show that in 3D geometry the Weibel instability persists even for collisionless background plasma. The anomalous plasma resistivity in 3D is caused by the two-stream instability.

DOI: 10.1103/PhysRevLett.101.255001 PACS numbers: 52.57.−z, 52.35.−g, 52.40.Mj, 52.65.Rr

The fast ignition (FI) fusion is a promising route towards laser-driven fusion. In the FI scheme [1], a laser-generated relativistic electron beam with a few MeV per electron energy must propagate and heat a hot spot in the core of a precompressed fusion fuel target. The current carried by these MeV electrons inside the plasma is much higher than the Alfvén current limit $I = 17\gamma$ kA, where γ is the Lorentz factor of the beam. Transportation of this electron beam is not possible unless it is compensated by a return plasma current. However, in this configuration, the current beam is subject to the Weibel and the two-stream instabilities. The Weibel instability [2] is one of the leading instabilities under relativistic conditions and has been studied for a long time [3–12]. Honrubia *et al.* [11] have performed three-dimensional simulations of resistive beam filamentation corresponding to the full scale FI configuration. Three-dimensional magnetic structures generated due to the Weibel instability in a collisionless plasma have also been reported [12]. Recently, the evidence of Weibel-like dynamics and the resultant filamentation of electron beams have been reported experimentally [6]. It was proposed in Ref. [7] that this instability could be suppressed by the transverse beam temperature alone in a collisionless plasma. However, the instability persists in the presence of collisions in return plasma current no matter how high the transverse beam temperature is. This regime of instability was termed the resistive beam instability [13].

In this Letter, we develop a theoretical model of the collisional Weibel instability in the framework of the quasineutrality assumption. It treats beam electrons as kinetic particles, and ambient plasma as a nonrelativistic fluid. For a finite-temperature beam, a new class of negative-energy magnetosound waves is identified. We derive conservation laws for the beam-plasma system and show that the energy of this system is not positively definite. Rather, it contains a negative term that allows for negative-energy waves. Collisions in the background plasma current excite unstable magnetosound waves in the system, which carry negative-energy densities. Because of these waves the Weibel instability is not suppressed even when the transverse beam temperature would be high enough to stabilize collisionless plasmas. We present results of detailed 2D and 3D particle-in-cell (PIC) simulations on the relativistic electron beam transport in plasmas. The 2D geometry corresponds to a plane transverse to the beam propagation direction. In this geometry the Weibel instability is decoupled from the two-stream instability. The simulation results show that the Weibel instability cannot be suppressed by thermal effects alone if collisions are present in the system. In 3D geometry, the simulation results show that the Weibel instability cannot be suppressed even in plasmas free from binary collisions. We conjecture that the effective collisions, leading to an anomalous resistivity in the return current, are provided by the turbulence emerging from the electrostatic beam instability.

We assume a very long electron beam propagating in the $\hat{z}$ direction and there is no dependence on the coordinate z. The beam and plasma densities are n_b and n_p, respectively, and the beam-plasma system is quasineutral, i.e., $n_b + n_p = n_0$, where n_0 is the background ion density. The strongest magnetic field is generated in the transverse plane (x-y plane). This magnetic field generates an axial component of the electric field E_z. The transverse components of the electric field are obtained from the force equilibration $\boldsymbol{E} + \boldsymbol{v}_{pz} \times \boldsymbol{B}_\perp/c = 0$, where $\boldsymbol{v}_{pz} = v_{pz}\boldsymbol{e}_z$ is the return plasma current velocity. To summarize, these are the dominant electric and magnetic fields of the beam-plasma system:

$$\boldsymbol{B}_\perp = -\boldsymbol{e}_z \times \boldsymbol{\nabla}_\perp A_z, \qquad E_z = -\frac{1}{c}\frac{\partial A_z}{\partial t}, \qquad \boldsymbol{E}_\perp = -(v_{pz}/c)\boldsymbol{\nabla}_\perp A_z, \tag{1}$$

where A_z is the z component of the vector potential. The B_z

component is small, but can be approximated using $\partial_t B_z = -(\nabla_\perp v_{pz} \times \nabla_\perp A_z) \cdot \boldsymbol{e}_z$. The A_z component is determined from the Ampere law

$$\nabla_\perp^2 A_z = -\frac{4\pi}{c}(J_{bz} + J_{pz}), \tag{2}$$

where J_{bz} and J_{pz} are the current densities of the beam and plasma, respectively. We discard the displacement current to ensure the quasineutrality. The axial equation of motion for the plasma flow and the transverse equations of motion for the beam electrons are

$$\frac{\partial v_{pz}}{\partial t} + \nu v_{pz} = \frac{e}{mc}\frac{\partial A_z}{\partial t}, \tag{3}$$

$$\frac{d(\gamma_j \boldsymbol{v}_{j\perp})}{dt} = -\frac{e(v_{jz} - v_{pz})}{mc}\nabla_\perp A_z, \tag{4}$$

where ν is the collisional frequency of the ambient plasma, m and c are the electron mass and velocity of light in vacuum, respectively, and the subscript j represents the jth beam electron. For a collisionless plasma, Eq. (4) is written as

$$\frac{d(\gamma_j \boldsymbol{v}_{j\perp})}{dt} = -\frac{e v_{jz}}{mc}\nabla_\perp A_z + \frac{e^2}{2m^2c^2}\nabla_\perp A_z^2. \tag{5}$$

The second term in the right-hand side of Eq. (5) is due to the extra pinching of the electron beam by the transverse electric field $\boldsymbol{E}_\perp$. We note here that $\boldsymbol{E}_\perp$ counters the magnetic expulsion of the ambient plasma. At the same time it reinforces the magnetic pinching of the beam. The generalized momentum conservation in the z direction gives

$$\gamma_j v_{jz} = \gamma_{j0} v_{jz0} + \frac{e}{mc}(A_z - A_{z0}). \tag{6}$$

If there is no dissipation, then we may derive conservation laws for the system. From Eqs. (2), (5), and (6), we have

$$\sum_j \gamma_j mc^2 - \sum_j \frac{m}{2}\left(\frac{eA_z}{mc}\right)^2 + \int d^2x L_z \frac{|\nabla A_z|^2}{8\pi} + \int d^2x L_z \frac{n_0 m}{2}\left(\frac{eA_z}{mc}\right)^2 = 0, \tag{7}$$

where L_z is the system length in the z direction. The first term in the above expression represents the total beam electron energy. The third and fourth terms correspond to the total magnetic energy and the plasma kinetic energy, respectively. The fourth term slightly overestimates the energy because the actual plasma density $n_p = n_0 - n_b$ is slightly smaller. The second term corrects this overcount: the excess energy is subtracted from the electron beam energy.

The relativistic treatment of the instability could be somewhat cumbersome. However, the essential physics can be learned from the nonrelativistic equation of motion. For a warm electron beam the equation of motion reads as

$$m\frac{d\boldsymbol{v}_{b\perp}}{dt} = -e\frac{v_{bz} - v_{pz}}{c}\nabla_\perp A_z - \frac{\nabla_\perp P}{n_b}, \tag{8}$$

where P is the beam pressure related to the beam emittance. Equation (8), on linearizing for small magnetic field perturbation, together with the continuity equation $\partial_t \delta n_b = -n_b(\nabla_\perp \cdot \delta \boldsymbol{v}_{b\perp})$, yields

$$\left(\frac{\partial^2}{\partial t^2} - c_s^2\nabla_\perp^2\right)\frac{\delta n_b}{n_b} = c^2\beta_0\nabla_\perp^2\tilde{A}_z, \tag{9}$$

where $\tilde{A}_z = eA_z/mc^2$, $\beta_0 = (v_{bz} - v_{pz})/c \approx v_{bz}/c$, $c_s^2 = 3v_{\rm th}^2$ is the square of the beam's sound speed, and it was assumed that $\nabla_\perp \delta P = 3v_{\rm th}^2 \nabla_\perp \delta n_b$. Equations (2), (3), and (9) form a set of equations to describe the sound like perturbation or filamentation of the electron beam density. The simplest case of collisionless plasma ($\nu = 0$) and long wavelength perturbation ($|k_\perp|^2 \ll \omega_{pe}^2/c^2$, ω_{pe} being the ambient plasma frequency) gives $(\partial^2/\partial t^2 - \bar{c}_s^2\nabla_\perp^2)\delta n_b/n_b = 0$, where $\bar{c}_s^2 = c_s^2 - c^2\beta_0^2 n_b/n_p$ is the modified sound speed. One may note that the cold beam ($c_s^2 < c^2\beta_0^2 n_b/n_p$) is unstable due to the Weibel instability whereas the warm beam is stable. For a warm beam the dispersion for sound waves is given by $\omega^2 = \bar{c}_s^2 k_\perp^2$. These waves are stable and the Weibel instability does not occur for sufficiently high transverse beam temperature and low beam/plasma density ratios. With finite plasma resistivity taken into account the dispersion relation for the sound waves reads as

$$\omega^2 = c_s^2 k_\perp^2 - \frac{\omega_b^2\beta_0^2 k_\perp^2}{(k_\perp^2 + k_{pe}^2/(1 + i\nu/\omega))}, \tag{10}$$

where ω_b is the beam-plasma frequency. For large scale perturbations ($k_\perp^2 \ll k_{pe}^2$, $k_{pe}^{-1} = c/\omega_{pe}$) and small collision frequency, Eq. (10) yields three modes

$$\omega \approx \pm\bar{c}_s|k_\perp| - i\nu\frac{c^2\beta_0^2 n_b}{2\bar{c}_s^2 n_p}, \tag{11}$$

and

$$\omega \approx i\nu\frac{c^2\beta_0^2 n_b}{2\bar{c}_s^2 n_p}. \tag{12}$$

The energy density associated with the last mode can easily be checked to be negative. Thus collisions drive negative-energy waves in the system, leading to the Weibel instability of a warm electron beam, which would be stable in collisionless plasmas.

We carry out detailed 2D PIC simulations to check the analytical findings. The relativistic electron beam propagates in the negative $\hat{z}$ direction with the initial velocity

v_{bz}. The compensating return current of the ambient plasma electrons flows with the initial velocity v_{pz}. The plasma ions are immobile and have the density $n_0 = n_b + n_p$. The simulation domain size is $X \times Y = (20\lambda_s \times 20\lambda_s)$, where $\lambda_s = c/\omega_{pe}$ is the plasma skin depth. All simulations are performed with 64 particles per cell and with a grid size of $\delta x = \delta y = 0.125\lambda_s$. The density ratio between the plasma and beam electrons is $n_p/n_b = 9$, whereas the beam and background plasma electrons have velocities $v_{bz} = 0.9c$ and $v_{pz} = -0.1c$. The binary collisions are simulated with a newly implemented collision module in the Virtual Laser Plasma Laboratory (VLPL) PIC code [14]. We record the evolution of field energy for every component F_i of the fields $\mathbf{E}$ and $\mathbf{B}$ as $\int_S (eF_i/mc\omega_{pe})^2 dxdy$. We take the electron beam with temperature $T_b \sim 70$ keV and the ambient plasma collision frequency $\nu/\omega_{pe} = 0.15$ for these simulations.

Figure 1 shows snapshots of the transverse $\mathbf{E}$ and $\mathbf{B}$ fields, and the structure of the beam filaments at a time, $T = 20(2\pi/\omega_{pe})$ for four different cases: (a) cold electron beam and collisionless background plasma, (b) cold electron beam and collisional background plasma, (c) hot electron beam and collisionless background plasma, and (d) hot electron beam and collisional background plasma. The beam density filamentation is shown in the last column in each panel. In collisionless case (a), the filaments are small, comparable with the plasma skin depth. In the collisional case (b), the filament size is bigger. This can be explained as a collisional diffusion of plasma electrons across the self-generated magnetic fields. In the third panel of figure, simulation case (c), the electron beam has the transverse temperature $T_b \sim 70$ keV, and the background plasma electrons are collisionless. Here we see no filament formation. The temperature of the electron beam stabilizes the Weibel instability. Physically the thermal pressure of the electron beam prevails over the magnetic pressure in this case. Hence, the magnetic field pinching which actually drives the instability does not occur, resulting in the suppression of the Weibel instability. The last panel of the figure depicts the filament formation in the simulation case (d). Although the beam temperature is the same as in the stable collisionless case (c), the background plasma collisions revive back the instability. This is due to the collisions induced generation of negative-energy waves as discussed earlier in the theoretical model.

Figure 2 shows the evolution of electric and magnetic field energies in the four cases corresponding to the simulations in Fig. 1. The energy axes in Fig. 2 use logarithmic scales. We see a stage of linear instability, where the field energies build up exponentially in time. It is followed by the nonlinear saturation later. The linear instability stage is present in the simulations (a), (b), and (d). The simulation case (c), where the electron beam had high temperature and the background plasma was collisionless, shows no linear stage of instability and no significant build up of the fields energies. The linear growth rates calculated from the simu-

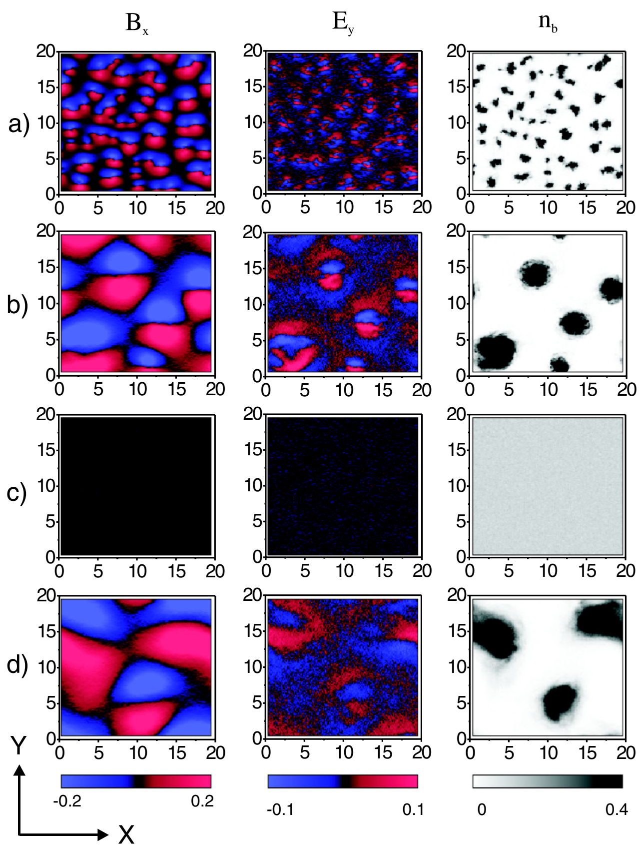

FIG. 1 (color online). Snapshots of the evolution of transverse electromagnetic fields (E_x and B_x) and beam filament densities (n_b) during the nonlinear stage at a time $T = 20(2\pi/\omega_{pe})$ for four different simulation cases. See text for explanations.

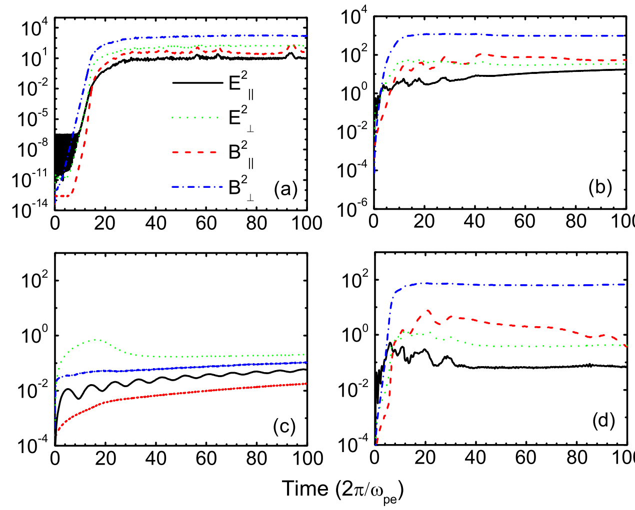

FIG. 2 (color online). Time evolution of the perpendicular and parallel field energies ($E^2_\perp$, $B^2_\perp$, $E^2_\parallel$, $B^2_\parallel$) for four different simulation cases as in Fig. 1.

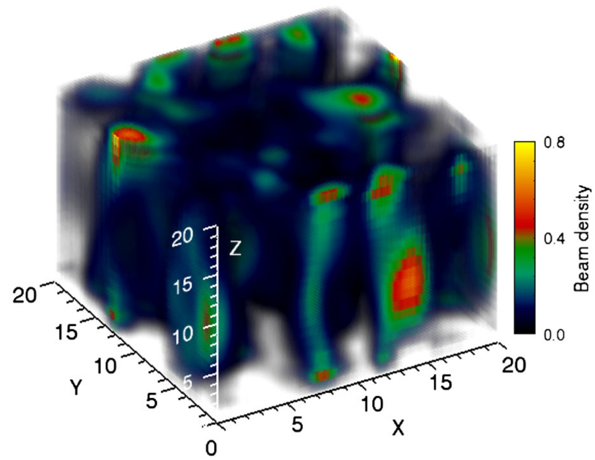

FIG. 3 (color online). Beam filaments from 3D PIC simulations corresponding to the case in Fig. 1(c).

lation results agree well with the theoretical model. After the linear stage of the instability, magnetic attraction of the filaments starts and the field energies saturate. Some small fluctuations around the saturated field energies can be seen. These fluctuations occur due to the collective merging of the filaments, also discussed in [9].

We have also done a number of 3D PIC simulations varying the beam temperature and the plasma collision frequency. To our surprise, we found no stabilization even in the collisionless case for high beam temperatures. The corresponding simulation is shown in Fig. 3. Although the electron beam in this simulation had the high transverse temperature, and the plasma had no binary collisions, we see a lot of filamentation due to the Weibel instability. We explain this fact in terms of anomalous plasma collisionality. Indeed, there is an oblique mode in the 3D geometry which couples the Weibel and the two-stream instabilities [8]. The two-stream mode generates electrostatic turbulence in the plasma. Stochastic fields associated with this turbulence scatter the beam and plasma electrons and lead to an effective collisionality in the return plasma current, which revives back the Weibel instability. It may be noted here that we have always taken the background plasma as cold. The interplay of collisions in different regimes of beam and background plasma temperatures can be found in Ref. [5].

In summary, we have developed a simplified model which identifies the collisional Weibel instability as the instability of the unstable negative-energy mode driven by collisions in the background plasma. An important result of this study is that beam temperature does not kill the Weibel instability in the presence of collisions in the beam-plasma system. Detailed 2D simulations on the Weibel instability of an electron beam have been performed, which essentially confirm the theoretical prediction. An alternate explanation on the persistence of the Weibel instability in 3D geometry is offered. It is attributed to the anomalous collisionality of the beam-plasma system due to the two-stream mode.

This work was supported by the DFG through TR-18 project and the U.S. Department of Energy Grants No. DE-FG02-04ER41321 and No. DE-FG02-04ER54763.

*pukhov@tp1.uni-duesseldorf.de

[1] M. Tabak *et al.*, Phys. Plasmas **1**, 1626 (1994).
[2] E. S. Weibel, Phys. Rev. Lett. **2**, 83 (1959).
[3] A. Pukhov and J. Meyer-ter-Vehn, Phys. Rev. Lett. **76**, 3975 (1996); M. V. Medvedev and A. Loeb, Astrophys. J. **526**, 697 (1999).
[4] R. Lee and M. Lampe, Phys. Rev. Lett. **31**, 1390 (1973); P. H. Yoon and R. C. Davidson, Phys. Rev. A **35**, 2718 (1987); A. Pukhov and J. Meyer-ter-Vehn, Phys. Rev. Lett. **79**, 2686 (1997); F. Califano, F. Pegoraro, and S. V. Bulanov, Phys. Rev. E **56**, 963 (1997); Y. Sentoku, K. Mima, S. Kojima, and H. Ruhl, Phys. Plasmas **7**, 689 (2000); L. Gremillet, G. Bonnaud, and F. Amiranoff, Phys. Plasmas **9**, 941 (2002); Y. Sentoku, K. Mima, P. Kaw, and K. Nishikawa, Phys. Rev. Lett. **90**, 155001 (2003); J. M. Hill, M. H. Key, S. P. Hatchett, and R. R. Freeman, Phys. Plasmas **12**, 082304 (2005); O. Polomarov *et al.*, Phys. Plasmas **14**, 043103 (2007).
[5] C. Deutsch, A. Bret, M. C. Firpo, and P. Fromy, Phys. Rev. E **72**, 026402 (2005); J. M. Wallace, J. U. Brackbill, C. W. Cranfill, D. W. Forslund, and R. J. Mason, Phys. Fluids **30**, 1085 (1987); M. Honda, Phys. Rev. E **69**, 016401 (2004); T. Okada and K. Niu, J. Plasma Phys. **23**, 423 (1980); **24**, 483 (1980); W. Kruer, S. Wilks, B. Lasinski, B. Langdon, R. Town, and M. Tabak, Bull. Am. Phys. Soc. **48**, 81 (2003).
[6] R. Jung *et al.*, Phys. Rev. Lett. **94**, 195001 (2005); M. Tatarakis *et al.* Phys. Rev. Lett. **90**, 175001 (2003); M. Wei *et al.* Phys. Rev. E **70**, 056412 (2004).
[7] L. O. Silva, R. A. Fonseca, J. W. Tonge, W. B. Mori, and J. M. Dawson, Phys. Plasmas **9**, 2458 (2002).
[8] A. Bret, M.-C. Firpo, and C. Deutsch, Phys. Rev. E **70**, 046401 (2004); Phys. Rev. Lett. **94**, 115002 (2005); Laser Part. Beams **24**, 27 (2006); A. Bret, L. Gremillet, D. Bénisti, and E. Lefebvre, Phys. Rev. Lett. **100**, 205008 (2008).
[9] M. Honda, J. Meyer-ter-Vehn, and A. Pukhov, Phys. Rev. Lett. **85**, 2128 (2000).
[10] J. J. Honrubia, M. Kaluza, J. Schreiber, G. D. Tsakiris, and J. Meyer-ter-Vehn, Phys. Plasmas **12**, 052708 (2005); J. J. Honrubia, C. Alfonsín, L. Alonso, B. Pérez, and J. A. Cerrada, Laser Part. Beams **24**, 217 (2006).
[11] J. J. Honrubia and J. Meyer-ter-Vehn, Nucl. Fusion **46**, L25 (2006).
[12] F. Califano, D. Del Sarto, and F. Pegoraro, Phys. Rev. Lett. **96**, 105008 (2006).
[13] K. Molvig, Phys. Rev. Lett. **35**, 1504 (1975).
[14] A. Pukhov, J. Plasma Phys. **61**, 425 (1999).